NGR-05-009-079

N 69 37290

NASA TMX 105799

The Modal Decomposition of Aperture Fields in Detection and Estimation of Incoherent Objects

Carl W. Helstrom

Department of Applied Physics and Information Science

University of California, San Diego; La Jolla, Calif. 92037

Abstract

A decomposition of the field at the aperture of an optical system in terms of the eigenfunctions of a certain integral equation is useful in analyzing the detectability of incoherent objects. The kernel of the integral equation is the mutual coherence function of the light from the object. The decomposition permits specification of the number of degrees of freedom in the aperture field contributing to detection of the object. Quantum-mechanically the coefficients of the modal decomposition become operators similar to the usual creation and annihilation operators for field modes. The optimum detector of the object is derived in terms of these operators. Specific detection probabilities are calculated for a uniform circular object whose light is observed at a circular aperture The modal decomposition is also applied to estimating the radiance distribution of the object plane.

Detection, resolution, and parameter estimation in the object space are the primary functions of an optical system. That space is usually taken to be a plane, the mapping of whose radiance distribution is an important type of parameter estimation. Detection and resolution, on the other hand, involve decisions among hypotheses about the object plane.[1,2]

The data upon which these decisions and estimates are based are the values of the electromagnetic field at the aperture A of the optical system, as observed during a finite interval (0, T). Lenses, stops, and photosensitive surfaces process the aperture field in such a way as to facilitate the decisions and estimates. The quality of the system can be measured by probabilities of correct decisions and mean-square errors in estimates of object parameters. These measures are instructively compared with the best values attainable by any system working with the same data. The ideal optical system that maximizes probabilities of correct decision or minimizes estimation errors is called the optimum system, and its structure can be determined by the methods of detection theory.[3,4]

When the object plane radiates incoherently, the analysis by detection theory employs a characteristic decomposition of the aperture field into spatial and temporal modes. The mode functions are the eigenfunctions of an integral equation whose kernel is the spatio-temporal mutual coherence function of the part of the aperture field generated by the object to be detected. The associated eigenvalues determine the detectability of the object through the probability distributions of the modal expansion coefficients. Generally only a finite number M_T of the eigenvalues are significantly different from zero, and only the field modes associated with them contribute substantially to detection. Thus M_T specifies the number of significant degrees of freedom in the aperture field relative to the detection of a certain object. For spectrally pure object light M_T can be factored into a number M of spatial degrees of freedom and a number M' of temporal degrees of freedom. The temporal factor M' is the product WT of the observation interval T and the bandwidth W of the object light.

When the light from the object possesses complete first-order coherence at the aperture, $M = 1$ and there is a single significant spatial mode. When the object is so large, on the other hand, that the coherence length of its light is much smaller than the diameter of the aperture, $M \gg 1$ and--as we shall see--the mode eigenvalues are proportional to values of the object radiance at sample points separated by a conventional resolution interval. If the aperture is provided with a lens to focus the light onto an image plane, each spatial mode, for $M \gg 1$, goes into a conventional resolution element of the image. Mapping the radiance of the object plane, furthermore, can be treated as estimating the eigenvalues of these spatial modes.

The eigenfunctions and eigenvalues of the mutual coherence function of the aperture field thus supply a precise meaning for the concept of informative degrees of freedom in the aperture field with respect to detection and resolution. There is a direct relation to the concept of degrees of freedom in an image, as treated by Toraldo di Francia and others.[5]

This paper will develop in some detail the modal decomposition of the aperture field and its application to the detection of an object and the estimation of the radiance distribution of the object plane. Associated with the spatio-temporal field modes are quantum-mechanical operators with much the same properties as the creation and annihilation operators in the usual form of field quantization.[6] Under normal conditions of observation, the operators for different modes commute, and the detection of an incoherent object can be based on the number of photons counted in each mode. Specific results are given for detecting a uniform circular object by observation of the field over a circular aperture.

The theory is developed for a scalar model of the electromagnetic field. Our results can be applied to ordinary unpolarized light by doubling the effective number M of spatial modes in the field at the aperture of the observing system.

I. The Modal Decomposition of the Aperture Field

The Field

In this section the electromagnetic field at the aperture will be treated classically, and for simplicity it will be taken as a scalar. The positive-frequency part of the field--or analytic signal--$\psi_+(\underset{\sim}{r}, t)$ is composed of a part $\psi_s(\underset{\sim}{r}, t)$ due to the object, when present, and a part $\psi_n(\underset{\sim}{r}, t)$ due to the background,

$$\psi_+(\underset{\sim}{r}, t) = \psi_s(\underset{\sim}{r}, t) + \psi_n(\underset{\sim}{r}, t). \tag{1.1}$$

The background field, or "noise", $\psi_n(\underset{\sim}{r}, t)$ is spatially and temporally white, its distribution being much broader in both frequency and direction than that of the object component, or "signal", $\psi_s(\underset{\sim}{r}, t)$.

Both signal and noise fields are circular-complex, spatio-temporal gaussian random processes.[7] The probability density functions describing them are specified completely by their mutual coherence functions

$$\tfrac{1}{2}\underset{\sim}{E}[\psi_n(\underset{\sim}{r}_1, t_1)\ \psi_n^*(\underset{\sim}{r}_2, t_2)] =$$

$$\varphi_n(\underset{\sim}{r}_1, t_1; \underset{\sim}{r}_2, t_2) = N'\delta(\underset{\sim}{r}_1 - \underset{\sim}{r}_2)\ \delta(t_1 - t_2), \tag{1.2}$$

$$\tfrac{1}{2}\underset{\sim}{E}[\psi_s(\underset{\sim}{r}_1, t_1)\ \psi_s^*(\underset{\sim}{r}_2, t_2)] = \varphi_s(\underset{\sim}{r}_1, t_1; \underset{\sim}{r}_2, t_2), \tag{1.3}$$

where $\underset{\sim}{E}$ stands for the statistical expectation and N' is the spatio-temporal spectral density of the background light. The mutual coherence function of the total field is $\varphi_n + \varphi_s$.

For convenience of discussion we assume the light from the object to be quasimonochromatic and spectrally pure, so that its mutual coherence function can be factored into spatial and temporal parts,

$$\varphi_s(\underset{\sim}{r}_1, t_1; \underset{\sim}{r}_2, t_2) = \varphi_s(\underset{\sim}{r}_1, \underset{\sim}{r}_2)\ \chi(t_1 - t_2) \exp i\Omega(t_1 - t_2), \tag{1.4}$$

where $\Omega = 2\pi c/\lambda$ is the central angular frequency of the object light, whose predominant wavelength is λ. The temporal autocovariance function $\chi(\tau)$ is normalized so that $\chi(0) = 1$, and the spatial part $\varphi_s(\mathbf{r}_1, \mathbf{r}_2)$--as in III--so that the illuminance at point $\mathbf{r}$ of the aperture due to the object is $\varphi_s(\mathbf{r}, \mathbf{r})/2\Omega^2 c$. The total energy received from the object during the interval (0, T) is

$$E_s = (2\Omega^2 c)^{-1} T \int_A \varphi_s(\mathbf{r}, \mathbf{r})\, d^2\mathbf{r}.$$

The spectral density of the object light is

$$X(\omega) = \int_{-\infty}^{\infty} \chi(\tau)\, e^{i\omega\tau}\, d\tau, \tag{1.5}$$

with angular frequencies ω referred to Ω. Its bandwidth W is conveniently defined by

$$W = \left[\int_{-\infty}^{\infty} X(\omega)\, d\omega/2\pi\right]^2 \Bigg/ \int_{-\infty}^{\infty} [X(\omega)]^2\, d\omega/2\pi = |\chi(0)|^2 \Bigg/ \int_{-\infty}^{\infty} |\chi(\tau)|^2 d\tau. \tag{1.6}$$

We shall assume, as is normal in practice, that the observation time T is much greater than the correlation time W^{-1} of the object light; $WT \gg 1$.

The Modal Expansion

In treating the optimum detection of a temporal gaussian stochastic process, or random signal, in the presence of white noise, it is convenient to decompose the input to the receiver in a Karhunen-Loève expansion, whose terms are the eigenfunctions of the autocovariance function of the signal.[9] The coefficients of the expansion are statistically independent gaussian random variables in both the presence and the absence of the signal.

A similar expansion is useful in analyzing the detectability of optical fields.[10] The aperture field is written as

$$\psi_+(\underset{\sim}{r}, t) = \sum_p \sum_m a_{pm} f_{pm}(\underset{\sim}{r}, t), \qquad (1.7)$$

where the a_{pm} are statistically independent gaussian random variables. The expansion functions $f_{pm}(\underset{\sim}{r}, t)$ are orthonormal over the aperture A and the interval (O, T),

$$\int_A \int_0^T f_{pm}^*(\underset{\sim}{r}, t) f_{qn}(\underset{\sim}{r}, t) d^2\underset{\sim}{r}dt = \delta_{pq} \delta_{mn}. \qquad (1.8)$$

They are eigenfunctions of the integral equation

$$\lambda_{pm} f_{pm}(\underset{\sim}{r}, t) = C \int_A d^2\underset{\sim}{s} \int_0^T du \, \varphi_s(\underset{\sim}{r}, t; \underset{\sim}{s}, u) f_{pm}(\underset{\sim}{s}, u) \qquad (1.9)$$

with C a suitable constant.

Because the object light is assumed spectrally pure, Eq. (1.4) permits us to break the eigenfunction $f_{pm}(\underset{\sim}{r}, t)$ into spatial and temporal factors,

$$f_{pm}(\underset{\sim}{r}, t) = \eta_p(\underset{\sim}{r}) \gamma_m(t) e^{-i\Omega t}, \qquad (1.10)$$

$$\lambda_{pm} = h_p g_m, \qquad (1.11)$$

where $\gamma_m(t)$ is an eigenfunction of $\chi(t - s)$,

$$g_m \gamma_m(t) = T^{-1} \int_0^T \chi(t - s)\, \gamma_m(s)\, ds \tag{1.12}$$

and $\eta_p(\underset{\sim}{r})$ an eigenfunction of $\varphi_s(\underset{\sim}{r}, \underset{\sim}{s})$,

$$h_p \eta_p(\underset{\sim}{r}) = (2\Omega^2 cT/E_s) \int_A \varphi_s(\underset{\sim}{r}, \underset{\sim}{s})\, \eta_p(\underset{\sim}{s})\, d^2\underset{\sim}{s}. \tag{1.13}$$

The constant C has been selected in such a way that Eq. (1.13) is equivalent to III, Eq. (5.6) with $h_p = \nu_p/N_s$, where N_s is the average total number of photons received from the object at the aperture A during the interval (0, T), and ν_p are the eigenvalues defined in III. Both sets of eigenfunctions sum to 1,

$$\sum_m g_m = 1, \qquad \sum_p h_p = 1, \tag{1.14}$$

and are considered as arranged in descending order.

The Temporal Integral Equation

Studying the temporal integral equation (1.12) briefly will help us understand the spatial one, Eq. (1.13). Since $WT \gg 1$, the width of the kernel $\chi(\tau)$ in Eq. (1.12) is much less than the length T of the interval of integration, and the spectral density $X(\omega)$ does not vary significantly as ω changes by $2\pi/T$. The eigenvalues are then approximately[11]

$$g_m \cong T^{-1} X(2\pi m/T), \; m = \ldots -2, -1, 0, 1, 2, \ldots \tag{1.15}$$

The number of eigenvalues significantly different from zero is of the order of WT. The associated eigenfunctions are approximately the complex exponentials,

$$\gamma_m(t) \cong T^{-1/2} \exp(-2\pi i m t/T). \tag{1.16}$$

The highest frequencies appearing in the significant temporal modes, as measured with respect to $\Omega/2\pi$, are of the order of W.

If the autocovariance function $\chi(\tau)$ were periodic in τ with period T, the eigenvalues and eigenfunctions would be given exactly by the right-hand sides of Eqs. (1.15) and (1.16), as substitution into Eq. (1.12) easily demonstrates. When the width W^{-1} of $\chi(\tau)$ is much less than T, the fact that $\chi(\tau)$ is not periodic, but is concentrated about $\tau = 0$, does not alter g_m and $\gamma_m(t)$ very much.

Since we are mainly concerned here with the spatial properties of the aperture field, we shall assume that the temporal spectral density $X(\omega)$ is constant over the range $-\pi W < \omega < \pi W$ and zero elsewhere. There are then WT eigenvalues equal approximately to $(WT)^{-1}$, and all the temporal modes specified by the $\gamma_m(t)$ are equivalent. The exact eigenfunctions are the prolate spheroidal wavefunctions,[12] and the exact eigenvalues are nearly $g_m \equiv (WT)^{-1}$ for $1 \le |m| \le \frac{1}{2}WT$. The g_m become very small for $m > WT$. In optics the product WT may be 10^5 or more.

The Spatial Integral Equation

We suppose that the object to be detected is very far away and subtends a small solid angle from the point of observation. Its radiance is given by the function $B(\underset{\sim}{u})$, in which $\underset{\sim}{u}$ is a 2-vector of coordinates in the object plane. Then it follows from the Fresnel-Kirchhoff approximation that the spatial coherence function at the aperture is[13]

$$\varphi_s(\underset{\sim}{r}_1, \underset{\sim}{r}_2) = (8\pi R^2 \Omega^2 c)^{-1} \exp\left[\frac{ik}{2R}(\underset{\sim}{r}_1{}^2 - \underset{\sim}{r}_2{}^2)\right] \beta(\underset{\sim}{r}_2 - \underset{\sim}{r}_1), \tag{1.17}$$

where $\beta(\underset{\sim}{r})$ is the Fourier transform of the object radiance,

$$\beta(\underset{\sim}{r}) = \int_O B(\underset{\sim}{u}) \exp(ik\underset{\sim}{u}\cdot\underset{\sim}{r}/R)\, d^2\underset{\sim}{u}. \tag{1.18}$$

Here O indicates an integration over the object plane, R is the distance to the object, and $k = 2\pi/\lambda$.

By defining new eigenfunctions

$$\eta_p'(\underset{\sim}{r}) = \eta_p(\underset{\sim}{r}) \exp(-ik\underset{\sim}{r}^2/2R), \tag{1.19}$$

we can write the spatial integral equation as

$$h_p \eta_p'(\underset{\sim}{r}_1) = [A\beta(0)]^{-1} \int_A \beta(\underset{\sim}{r}_2 - \underset{\sim}{r}_1)\, \eta_p'(\underset{\sim}{r}_2)\, d^2\underset{\sim}{r}_2, \tag{1.20}$$

where A is the area of the aperture. The spatial integral equation has now the convolutional form of the temporal one, Eq. (1.12). The function $\beta(\underset{\sim}{r})$ corresponds to $\chi(\tau)$, the radiance $B(\underset{\sim}{u})$ to the spectal density $X(\omega)$.

When the object is a "point", that is, when it subtends from the aperture a solid angle much less than λ^2/A, the object field possesses first-order coherence over the aperture, $\beta(\underset{\sim}{r}) \equiv \beta(0)$. There is a single eigenvalue h_1 equal to 1, and the rest of the eigenvalues h_p are zero. The eigenfunction $\eta_1'(\underset{\sim}{r})$ associated with h_1 is constant, $\eta_1'(\underset{\sim}{r}) \equiv A^{-1/2}$. The remaining eigenfunctions can be an arbitrary set of functions orthonormal among themselves and to $\eta_1'(\underset{\sim}{r})$. Only a single field mode at the aperture is significant for detecting a point object or for estimating its radiance or its frequency.[14]

When the object is so large that its solid angle spans many multiples of λ^2/A, and when its radiance $B(\underset{\sim}{u})$ varies only slightly over distances of the order of $\lambda RA^{-\frac{1}{2}}$, the widths of the mutual coherence function and $\beta(\underset{\sim}{r})$ are much smaller than the diameter of the aperture. The eigenvalues h_p can then be approximated in the same manner as the g_m's in Eq. (1.12), provided the aperture is rectangular. We denote its length by a, its width by b; its area is A = ab. The integral equation (1.20) is now a two-dimensional version of Eq. (1.12). The mode subscripts become 2-vectors $\underset{\sim}{p} = (p_x, p_y)$ of integers p_x and p_y to account for the x- and y-directions.

The eigenvalues $h_{\underset{\sim}{p}}$ are now approximately

$$h_{\underset{\sim}{p}} \cong A_\delta \, B(p_x\delta_x, \, p_y\delta_y)/B_T, \tag{1.21}$$

where $\delta_x = \lambda R/a$, $\delta_y = \lambda R/b$, and $A_\delta = \delta_x\delta_y$. Here

$$B_T = \beta(0) = \int_O B(\underset{\sim}{u}) \, d^2\underset{\sim}{u} \tag{1.22}$$

is the integrated radiance of the object. The eigenfunction associated with $h_{\underset{\sim}{p}}$ is approximately

$$\eta_{\underset{\sim}{p}}'(\underset{\sim}{r}) \cong A^{-\frac{1}{2}} \exp[2\pi i(p_x x a^{-1} + p_y y b^{-1})]. \tag{1.23}$$

The eigenfunctions $\eta_{\underset{\sim}{p}}'(\underset{\sim}{r})$ depend only weakly on the actual distribution $B(\underset{\sim}{u})$ of the radiance, provided $B(\underset{\sim}{u})$ nowhere changes by very much over distances of the order of δ_x and δ_y.

When the area A_o of the object is so large that $A_o/\delta_x\delta_y >> 1$, the eigenvalues $h_{\underset{\sim}{p}}$ are proportional to samples of the object radiance at points separated in x by $\delta_x = \lambda R/a$ and in y by $\delta_y = \lambda R/b$. The area $A_\delta = \delta_x\delta_y$ associated with each sampling point subtends from the aperture a solid angle of $A_\delta/R^2 = \lambda^2/A$. The number of significant spatial modes in the aperture field is roughly equal to $M = A_o/A_\delta = AA_o/\lambda^2R^2$. The highest spatial frequencies occurring in the significant modes are of the order of $a_o/\lambda R$ and $b_o/\lambda R$ in the x- and y-directions, where a_o and b_o are the length and breadth of the object. These spatial frequencies will be much less than $k/2\pi = \lambda^{-1}$ when $A_o << R^2$, that is, when the solid angle A_o/R^2 subtended by the object is much less than 1 steradian.

If a lens of focal length F is placed in the aperture, it focuses the object plane onto an image plane at a distance $R' = RF/(R + F)$ beyond the aperture. The component of the aperture field proportional to $\eta_p(\tilde{r})$ creates at point (x', y') in the image plane a field proportional to

$$\mathrm{sinc}[\pi(x' - \xi_{px})/\delta_x'] \; \mathrm{sinc}[\pi(y' - \xi_{py})/\delta_y'],$$
$$\delta_x' = \lambda R'/a, \; \delta_y' = \lambda R'/b,$$

where

$$(\xi_{px}, \xi_{py}) = (p_x\delta_x', p_y\delta_y')$$

is the geometrical image of the object point $(p_x\delta_x, p_y\delta_y)$, and $\mathrm{sinc}\, x = (\sin x)/x$. Thus each spatial mode of the aperture field generates in the image plane the diffracted image of its associated object point. When $M = A_o/\delta_x\delta_y >> 1$, the mode expansion of the aperture field corresponds to the usual expansion of the field in the image plane through the Whittaker-Shannon sampling theorem.[15]

In this way the integral equations (1.13) and (1.20) permit a measure of the number of spatial degrees of freedom in the aperture field that contribute to detection and estimation of the object. The measure reduces to the generally accepted one at both extremes of complete first-order coherence ($A_o/\delta_x\delta_y << 1$) and extreme incoherence ($A_o/\delta_x\delta_y >> 1$), yet is definable through Eqs. (1.13) and (1.20) for intermediate degrees of first-order coherence as well.

Circular Aperture

For a circular aperture a general sampling approximation similar to Eq. (1.21) has not been discovered. If the radiance distribution of the object possesses circular symmetry, $B(\underset{\sim}{u}) = B(|\underset{\sim}{u}|)$, however, the eigenvalues are given approximately by

$$h_{kn} = (\lambda^2 R^2/AB_T)\ B(x_{km}\lambda R/2\pi a), \tag{1.24}$$

where a is the radius of the aperture and the numbers x_{kn} are the zeros of the Bessel function of order n,

$$J_n(x_{kn}) = 0, \quad k = 0, 1, 2, 3, \ldots \quad . \tag{1.25}$$

For n = 0 the eigenvalues have multiplicity 1, for m > 0 multiplicity 2. The derivation is presented in Appendix A.

When the object is a circle of area $A_o = \pi a_o^2$ radiating uniformly, the integral equation (1.20) reduces to the one treated by Slepian.[16] The mode functions $\eta_{kn}'(\underset{\sim}{r})$ are proportional to the generalized prolate spheroidal wave functions, and the associated eigenvalues are

$$h_{kn} = (4/\alpha^2)\ \lambda_{n,k}(\alpha),$$
$$\alpha = kaa_o/R = 2\pi aa_o/\lambda R, \tag{1.26}$$

where $\lambda_{n,k}$ are the eigenvalues tabulated by Slepian; our α corresponds to his parameter c. For $\alpha >> 1$ the number of significant eigenvalues is approximately

$$M = \alpha^2/4 = AA_o/\lambda^2 R^2, \tag{1.27}$$

those of multiplicity 2 being counted twice. The significance of the generalized prolate spheroidal wave functions for representing the field in the image plane has been pointed out by Toraldo di Francia.[5]

As Slepian has shown,[16] the eigenvalues $\lambda_{n,k}(\alpha)$ are small for $\alpha << 1$ and approach 1 exponentially when $\alpha >> 1$. According to Eq. (1.24), an eigenvalue $\lambda_{n,k}(\alpha)$ will be significantly large when the parameter α exceeds the corresponding zero x_{kn} of the Bessel function $J_n(x)$. For $\alpha = 10$, for instance, there are $2 \times 9 + 3 = 21$ zeros x_{kn} less than α, counting zeros with $n > 0$ twice. Of the corresponding eigenvalues $\lambda_{n,k}(10)$ the smallest is $\lambda_{6,0}(10) = 0.740$. For $\alpha = 10$, $M = \alpha^2/4 = 25$.

II. Quantum Detection

The Mode Operators

The decomposition of the aperture field into spatio-temporal modes can be used, as indicated by Kuriksha,[17] to derive the optimum detector of the light from an incoherently radiating object in the presence of thermal background light. The principal assumptions required are that the light from the object fall nearly perpendicularly upon the aperture from a cone of directions much narrower than 1 steradian and that the diameter of the aperture be much greater than the correlation length of the thermal light and the wavelength of the object light.

Quantum-mechanically the field at the aperture is treated as an operator. It is divided into its positive-frequency part $\psi_+(\tilde{r}, t)$ and its negative-frequency part $\psi_-(\tilde{r}, t)$, which are hermitian conjugate operators,

$$\psi_-(\tilde{r}, t) = [\psi_+(\tilde{r}, t)]^+. \tag{2.1}$$

Classically $\psi_+(\tilde{r}, t)$ corresponds to the analytic signal. The mutual coherence function of the aperture field is

$$\varphi(\tilde{r}_1, t_1; \tilde{r}_2, t_2) = \mathrm{Tr}[\rho\psi_-(\tilde{r}_2, t_2)\ \psi_+(\tilde{r}_1, t_1)], \tag{2.2}$$

where Tr stands for the trace and ρ is the density operator of the field.[8] When the object is present, φ is the sum of φ_s and φ_n as given by Eqs. (1.2) and (1.3); when the object is absent, $\varphi = \varphi_n$.

The field operator $\psi_+(r, t)$ is expanded in the spatio-temporal modes defined by Eqs. (1.10) and (1.11). The coefficients of this expansion are proportional to the quantum-mechanical operators

$$b_{\tilde{p}m} = (2\Omega c/\hbar)^{1/2} \int_A \int_0^T e^{i\Omega t}\ \eta_{\tilde{p}}^*(\tilde{r})\ \gamma_m^*(t)\ \psi_+(\tilde{r}, t)\ d^2\tilde{r}dt. \tag{2.3}$$

In the expansion of $\psi_-(\underset{\sim}{r}, t)$ the hermitian conjugate operators

$$b_{\underset{\sim}{q}n}{}^{+} = (2\Omega c/\hbar)^{1/2} \int_A \int_0^T e^{-i\Omega t}\, \eta_{\underset{\sim}{q}}(\underset{\sim}{r})\, \gamma_n(t)\, \psi_-(\underset{\sim}{r}, t)\, d^2\underset{\sim}{r}dt \qquad (2.4)$$

appear. Under the assumptions stated at the beginning, these operators commute for different spatio-temporal modes; specifically, their commutators are

$$[b_{\underset{\sim}{p}m}, b_{\underset{\sim}{q}n}{}^{+}] = b_{\underset{\sim}{p}m}b_{\underset{\sim}{q}n}{}^{+} - b_{\underset{\sim}{q}n}{}^{+}b_{\underset{\sim}{p}m} = \delta_{\underset{\sim}{p}\underset{\sim}{q}}\delta_{mn},$$

$$[b_{\underset{\sim}{p}m}, b_{\underset{\sim}{q}n}] = [b_{\underset{\sim}{p}m}{}^{+}, b_{\underset{\sim}{q}n}{}^{+}] = 0. \qquad (2.5)$$

These operators play the same role as the ordinary creation and annihilation operators for the spatial modes of the electromagnetic field when quantized in a closed volume.[6,18]

To derive the first of these commutation relations, the commutator of the operators $\psi_+(\underset{\sim}{r}_1, t_1)$ and $\psi_-(\underset{\sim}{r}_2, t_2)$ is used; it is proportional to the positive-frequency part of Green's function for the free scalar field,[18]

$$[\psi_+(\underset{\sim}{r}_1, t_1), \psi_-(\underset{\sim}{r}_2, t_2)] =$$

$$\tfrac{1}{2}\hbar(2\pi)^{-3}\iiint \omega^{-1} \exp[-i\omega(t_1 - t_2) + i\underset{\sim}{k}\cdot(\underset{\sim}{r}_1 - \underset{\sim}{r}_2)]\, d^3\underset{\sim}{k},$$

$$\omega^2 = c^2\underset{\sim}{k}^2 = c^2(k_x{}^2 + k_y{}^2 + k_z{}^2). \qquad (2.6)$$

Using Eqs. (2.3), (2.4), and (2.6), we find

$$[b_{\underset{\sim}{p}m}, b_{\underset{\sim}{q}n}{}^{+}] = (\Omega/8\pi^3 c) \int_A\int_0^T \int_A\int_0^T \iiint |k_z|^{-1}\, \eta_{\underset{\sim}{p}}{}^*(\underset{\sim}{r}_1)\, \gamma_m{}^*(t_1)$$

$$\times\, \eta_{\underset{\sim}{q}}(\underset{\sim}{r}_2)\, \gamma_n(t_2)\, \exp[i(\Omega - \omega)(t_1 - t_2) + i\underset{\sim}{k}\cdot(\underset{\sim}{r}_1 - \underset{\sim}{r}_2)]$$

$$\times\, d^2\underset{\sim}{r}_1 d^2\underset{\sim}{r}_2 dt_1 dt_2 dk_x dk_y d\omega. \qquad (2.7)$$

In the process we have changed integration variables from (k_x, k_y, k_z) to (k_x, k_y, ω), with $\omega d\omega = c^2|k_z|dk_z$. In Eq. (2.7),

$$\underset{\sim}{k} \cdot (\underset{\sim}{r}_1 - \underset{\sim}{r}_2) = k_x(x_1 - x_2) + k_y(y_1 - y_2),$$

z_1 and z_2 having been set equal to 0 for points on the aperture.

The right-hand side of Eq. (2.7) contains the Fourier transforms of $\gamma_m^*(t_1)$ and $\gamma_n(t_2)$. We have seen in Section I that the largest frequencies in these functions are of the order of W. Hence in the integration over ω in Eq. (2.7) a significant contribution will be made only by values of ω within about W of Ω, and $W \ll \Omega$. The multiple integral also contains the spatial Fourier transforms of $\eta_{\underset{\sim}{p}}^*(\underset{\sim}{r}_1)$ and $\eta_{\underset{\sim}{q}}(\underset{\sim}{r}_2)$. The highest spatial frequencies in these functions are much less than $k = 2\pi/\lambda$ when, as assumed, the object subtends a solid angle much less than 1 steradian. Hence, to the integration over k_x and k_y in Eq. (2.7) only values of k_x and k_y much less than $k = \omega/c$ contribute. It is therefore an accurate approximation to set

$$|k_z| = (\omega^2 c^{-2} - k_x^2 - k_y^2)$$

equal to Ω/c and take it outside the integral. The integrations over ω, k_x, and k_y now lead to delta-functions, and when these are integrated out and the orthonormality of the mode functions is used, the first part of Eq. (2.5) results. The second part follows immediately from the commutator

$$[\psi_+(\underset{\sim}{r}_1, t_1), \psi_+(\underset{\sim}{r}_2, t_2)] = 0$$

and its hermitian conjugate.

The mode operators $b_{\underset{\sim}{p}m}$, $b_{\underset{\sim}{q}n}^+$ are not ordinary quantum-mechanical operators because they possess no time dependence. They are determined, as in Eqs. (2.3) and (2.4), by integrals of the aperture field over two spatial dimensions and over time. Despite this unusual character, the operators for different modes are in principle measurable simultaneously. In back of the aperture a large, lossless cavity is placed, as described in III. Initially empty, it is exposed to the aperture field during the interval (0, T), after which it is closed.

The operators $\tilde{b}_{pm}$ and $\tilde{b}_{qn}^{+}$ can be expressed as linear combinations of the creation and annihilation operators of the cavity modes at any later time $t > T$ by applying the technique developed in III. Since $\tilde{b}_{pm}$ and $\tilde{b}_{qn}^{+}$ commute, so do those linear combinations and are hence measurable by suitable observations of the cavity field.

The Optimum Detector

Both the object and the background contain a great many atoms, ions, and electrons radiating independently. The density matrices ρ_0 and ρ_1 describing the field under the two hypotheses H_0 (object absent) and H_1 (object present) have, therefore, gaussian P-representations.[19] These depend only on the mode correlation matrices $\mathrm{Tr}(\rho_i b_{\underset{\sim}{qn}}^{+} b_{\underset{\sim}{pm}})$, i = 0, 1, which are related through Eqs. (2.3) and (2.4) to the mutual coherence functions of the aperture field under H_0 and H_1.

Because the diameter of the aperture is much greater than the correlation length of the background field, and because the rays from the object are paraxial, the mutual coherence function φ_n of the background light can be expressed in the delta-function form of Eq. (1.2), as discussed in III, Section IV. Furthermore, the mode functions are eigenfunctions of the mutual coherence function of the object light, Eq. (1.9). As a consequence of Eqs. (1.2) and (1.9) and of the orthonormality of the mode functions--Eq. (1.8)--, the mode correlation matrices $\mathrm{Tr}(\rho_i b_{\underset{\sim}{qn}}^{+} b_{\underset{\sim}{pm}})$ under both hypotheses are diagonal. The modes are statistically independent and can be treated separately. Furthermore, the density matrices ρ_0 and ρ_1 now depend only on the number operators $n_{\underset{\sim}{pm}} = b_{\underset{\sim}{pm}}^{+} b_{\underset{\sim}{pm}}$ of the modes, and because of Eq. (2.5) these commute and are simultaneously measurable.

The operator $n_{\underset{\sim}{pm}}$ determines the excitation level or number of photons in the spatio-temporal mode $(\underset{\sim}{pm})$. The outcome $n'_{\underset{\sim}{pm}}$ of a measurement of $n_{\underset{\sim}{pm}}$ is an integral-valued random variable with an exponential distribution,[19,20]

$$p_i(n'_{\underset{\sim}{pm}}) = (1 - v_{\underset{\sim}{pm}}^{(i)}) \exp(n'_{\underset{\sim}{pm}} \ln v_{\underset{\sim}{pm}}^{(i)}),$$

$$v_{\underset{\sim}{pm}}^{(i)} = N_{\underset{\sim}{pm}}^{(i)} / (N_{\underset{\sim}{pm}}^{(i)} + 1), \quad i = 0, 1, \tag{2.8}$$

where

$$N_{\underset{\sim}{p}m}^{(0)} = \mathfrak{N} = [\exp(\hbar\Omega/K\mathcal{T}) - 1]^{-1} \tag{2.9}$$

and

$$N_{\underset{\sim}{p}m}^{(1)} = \mathfrak{N} + h_{\underset{\sim}{p}} g_m N_s . \tag{2.10}$$

Here K is Boltzmann's constant, $\mathcal{T}$ is the effective absolute temperature of the background light, and $N_s = E_s/\hbar\Omega$ is the average total number of photons received at the aperture A from the object during (0, T). It has been assumed in Eq. (2.9) that all significant modes have the same frequency Ω; the differences are at most of the order of $W \ll \Omega$.

The independence of the modes permits basing the optimum detector on the logarithmic likelihood ratio[4]

$$U = \ln \prod_{\underset{\sim}{p},m} p_1(n'_{\underset{\sim}{p}m})/p_0(n'_{\underset{\sim}{p}m}) =$$

$$\sum_{\underset{\sim}{p},m} \{n'_{\underset{\sim}{p}m} \ln(v_{\underset{\sim}{p}m}^{(1)}/v_{\underset{\sim}{p}m}^{(0)}) + \ln[(1 - v_{\underset{\sim}{p}m}^{(1)})/(1 - v_{\underset{\sim}{p}m}^{(0)})]\}. \tag{2.11}$$

The detector chooses H_1, deciding that the object is present, if U exceeds a decision level U_0, which can be set to provide a pre-assigned false-alarm probability

$$Q_0 = \Pr(U > U_0|H_0).$$

In the quantum limit $N_{\underset{\sim}{p}m}^{(1)} \ll 1$, $\mathfrak{N} \ll 1$, and $v_{\underset{\sim}{p}m}^{(i)} \doteq N_{\underset{\sim}{p}m}^{(i)}$, whereupon the logarithmic likelihood ratio is approximately

$$U = \sum_{\underset{\sim}{p},m} [n'_{\underset{\sim}{p}m} \ln(1 + h_{\underset{\sim}{p}} g_m N_s/\mathfrak{N}) - h_{\underset{\sim}{p}} g_m N_s]. \tag{2.12}$$

If, as we are generally assuming, the spectral density of the object light is uniform over a frequency interval of width W about $\Omega/2\pi$, and $WT \gg 1$, the eigenvalues g_m can be set equal to $(WT)^{-1}$, and the statistic U can be written as a sum over only spatial modes,

$$U = \sum_{\underset{\sim}{p}} [n_{\underset{\sim}{p}} \ln(1 + h_{\underset{\sim}{p}} N_s/\mathfrak{N}WT) - h_{\underset{\sim}{p}} N_s], \tag{2.13}$$

where

$$n_{\underset{\sim}{p}} = \sum n'_{\underset{\sim}{p}m} \tag{2.14}$$

is the total number of photons counted in spatial mode $\underset{\sim}{p}$ during (0, T). The optimum detector weights these numbers logarithmically in accordance with the expected number $N_{\underset{\sim}{p}s} = h_{\underset{\sim}{p}} N_s$ of photons received in that mode from the object when present.

When the object is a point source, only a single spatial mode is significant, and the decision can be based on the total number n_1 of photons counted at the aperture. Since $WT >> 1$, that number has a Poisson distribution under both hypotheses H_0 and H_1. The probability $Q_d = Pr\{U > U_0 | H_1\}$ of detecting the object can be calculated as described in III, Section V, where Q_d is plotted as a function of the average number N_s of signal photons for various values of $N_0 = \mathfrak{N}WT$.

When the object is extensive, $A_o/\delta_x\delta_y >> 1$, yet $A_o << R^2$, focusing the object plane onto an image plane associates each significant spatial mode $\eta_{\underset{\sim}{p}}(\underset{\sim}{r})$ in the aperture with a diffraction pattern in the image plane. The pattern is centered at the geometrical image of the associated object point $(p_x \delta_x, p_y \delta_y)$. Suppose the image plane to contain a mosaic of photosensitive spots just coinciding with the central peaks of each of these diffraction patterns. If their quantum efficiency equaled 1, the number of photoelectrons each spot emitted would be nearly equal to the number $n_{\underset{\sim}{p}}$ for the associated spatial mode, and a detector that weighted those numbers of photoelectrons as in Eq. (2.13) would be nearly equivalent to the optimum detector. Such a detector has been analyzed previously.[21]

The Threshold Detector

The optimum detector specified by Eq. (2.13) and depending through N_s on the total radiant power B_T of the object does not provide a uniformly most powerful test.[22] It must be set up for a standard object of radiance proportional to $B(\underset{\sim}{u})$ and total power $B_T^{(0)}$, and it will provide suboptimum detection of objects of different total power B_T.

A detector that is independent of knowledge of B_T, yet nearly as good as the optimum, is obtained by replacing the logarithm in Eq. (2.12) by the first term of its Taylor expansion. The constant factor $N_s/\mathfrak{N}$ can be cancelled from both statistic and decision level, and the new detector is equivalent to one basing its decision on the operator

$$U' = \sum_{\underset{\sim}{p},m} h_{\underset{\sim}{p}} g_m n_{\underset{\sim}{p}m} = \sum_{\underset{\sim}{p},m} h_{\underset{\sim}{p}} g_m b_{\underset{\sim}{p}m}^{+} b_{\underset{\sim}{p}m}. \tag{2.15}$$

This is the threshold detector derived in III. By using the definitions in Eqs. (2.3) and (2.4) and the orthonormality of the mode functions, U' can be written as a bilinear integral form in the field operators $\psi_-(\underset{\sim}{r}, t)$ and $\psi_+(\underset{\sim}{r}, t)$, with a result differing only by an inconsequential constant factor from III, Eq. (4.18). When $g_m \equiv (WT)^{-1}$, the threshold detector bases its decisions on the weighted sum

$$U'' = \sum_{\underset{\sim}{p}} h_{\underset{\sim}{p}} n_{\underset{\sim}{p}} \tag{2.16}$$

of the numbers $n_{\underset{\sim}{p}}$ of photons counted in the spatial modes $\underset{\sim}{p}$ during the interval (0, T).

When M = 1, the threshold and optimum detectors are identical, basing their decisions on the total number n_1 of photons observed at the aperture. When M >> 1, as we have seen, there are about M spatial modes with nearly equal eigenvalues $h_{\underset{\sim}{p}} \cong M^{-1}$, and both the threshold and the optimum detectors sum the numbers $n_{\tilde{p}}$ of photons in these modes with approximately a uniform weighting. The two detectors differ only in their treatment of modes whose eigenvalues are rather less than M^{-1}, and these contribute relatively little to the statistics U or U''. Hence, when their decision levels are adjusted to provide equal false-alarm probabilities Q_0, the threshold and the optimum detectors attain nearly the same probability of detection.

Detectability of a Circular Object

When the object radiates uniformly over a circle of radius a_0 and the aperture is a circle of radius a, the eigenvalues $h_p = h_{kn}$ determining the detection statistic and the probability of detection are given by Eq. (1.26) in terms of the eigenvalues tabulated by Slepian.[16] To illustrate the dependence of the probability of detection on the degree of coherence of the object light reaching the aperture, we have calculated it for the threshold detector,

$$Q_d = \Pr\{U'' > U_0 | H_1\},$$

as a function of the average total number N_s of photons from the object. The decision level U_0 was set to attain a false-alarm probability

$$Q_0 = \Pr\{U'' > U_0 | H_0\}$$

equal to 0.01, and the value of $N_0 = \mathfrak{N}WT$ was set equal to 1.0. The results are plotted in Fig. 1 for various values of $\alpha = 2\pi a a_0/R\lambda$.

For $\alpha = 0$ a single spatial mode contributes to the detection, and the optimum and threshold detectors are the same. The number of photons observed has a Poisson distribution, and the detection probability is calculated by III, Eqs. (5.17) - (5.19). For $\alpha = 1$ four terms and for $\alpha = 2$ five terms in the sum in Eq. (2.16) were used, corresponding to the four or five largest eigenvalues h_{kn}, and a computer was programmed to add up the joint Poisson probabilities of all sets of numbers $\underset{\sim}{n_p}$ for which the sum U'' is less than U_0; Q_d is equal to 1 minus this total probability. Taking seven terms for $\alpha = 2$ changed the detection probabilities only slightly, but greatly increased computation time.

For $\alpha \geqslant 4$ the moment-generating function (m. g. f.) of the statistic U'',

$$\mu(s; N_s) = \underset{\sim}{E}\,[\exp(sU'') | H_1] =$$

$$\exp\left[\sum_{k,n} (N_0 + N_s h_{kn}) \exp(h_{kn} s)\right], \tag{2.17}$$

was used to calculate the detection probability. The false-alarm probability Q_0 is the inverse Laplace transform of $[1 - \mu(-s; 0)]/s$ evaluated at $U' = U_0$, and this was approximated by the method of steepest descent, as in III, Eq. (5.23). By means of Newton's method the decision level U_0 yielding $Q_0 = 0.01$ was determined. The detection probabilities were then computed by summing the Gram-Charlier series,[23] whose coefficients are calculated by expanding $\ell n\, \mu(s; N_s)$ in a power series at $s = 0$. Terms in the series were summed as long as they decreased, and the summation was stopped when the terms began to increase again, consistently with the asymptotic nature of the Gram-Charlier series.

In order to compare the threshold detector with the optimum, the detection probabilities attained by the latter were also calculated for $\alpha = 4$, 6, and 8. The optimum detector was set up for a standard number $N_s^{(0)}$ of signal photons equal to 8; $N_0 = \mathfrak{N}WT = 1$. The moment-generating function for the optimum statistic U is the same as in Eq. (2.17), except that $\exp(h_{km}s)$ is replaced by $\exp[s\, \ell n\, (1 + N_s^{(0)} h_{km}/N_0)]$, and the same method of computation was used. The differences between the detection probabilities for the optimum and threshold detectors were of the order of the inaccuracy in the numerical calculations and too small to show up on the graph in Fig. 1.

The results demonstrate the slight difference between the performances of the optimum and the threshold detectors, and they show how, for a fixed false-alarm probability Q_0, the detection probability decreases as the object light is divided among more and more spatially incoherent degrees of freedom.

Detectability of Large Objects

The logarithm of the moment-generating function of the threshold operator U' in Eq. (2.15) is

$$\ell n\ \mu(s) = \underset{\sim}{E}(e^{sU'}\ |H_1) =$$

$$-\sum_{\underset{\sim}{p},m} \ell n\{1 - N^{(1)}_{\underset{\sim}{p}m}\ [\exp(h_{\underset{\sim}{p}} g_m s) - 1]\} \tag{2.18}$$

with the mean value $N^{(1)}_{\underset{\sim}{p}m}$ given by Eq. (2.10). Since $N^{(1)}_{\underset{\sim}{p}m} << 1$ under quantum-limited conditions, this is approximately

$$\ell n\ \mu(s) = \sum_{\underset{\sim}{p},m} (\mathfrak{N} + h_{\underset{\sim}{p}} g_m N_s)\ [\exp(h_{\underset{\sim}{p}} g_m s) - 1]. \tag{2.19}$$

When the object contains many degrees of freedom, MWT >> 1, the sum over the spatio-temporal modes can be replaced by an integration over temporal frequency and over the object by substituting from Eqs. (1.15) and (1.21). The result is

$$\ell n\ \mu(s) = \mathfrak{N} MT \int_O\int (d^2\underset{\sim}{u}/A_o)\int_{-\infty}^{\infty} (d\omega/2\pi)$$

$$\times\ [1 + N_s\ B(\underset{\sim}{u})\ X(\omega)/\bar{B}\mathfrak{N} MT]$$

$$\times\ \{\exp[B(\underset{\sim}{u})\ X(\omega)s/\bar{B}MT] - 1\}, \tag{2.20}$$

where $\bar{B} = B_T/A_o$ is the average radiance of the object and $M = AA_o/\lambda^2R^2$ is its effective number of degrees of freedom. This corresponds to III, Eq. (5.14) for a point object of arbitrary spectral density $X(\omega)$. An expansion of $\ell n\ \mu(s)$ in powers of s yields the cumulants of the distribution of the statistic U', from which the coefficients of the Gram-Charlier series can be calculated.[23] An example of a point object with a Lorentz spectrum was described in III, Section V.

III. Estimation of Object Radiance

We have seen in Section I that the eigenvalues $h_{\tilde{p}}$ of the spatial modes are proportional to samples of the radiance distribution $B(\tilde{u})$ of the object when the aperture is rectangular and the object so large that $M = AA_o/\lambda^2R^2 >> 1$. The mode functions are in this approximation independent of the actual form of $B(\tilde{u})$. The aperture field can therefore be expanded in spatial modes without knowledge of the true distribution of radiance in the object plane, and the strength of each mode in the component of the aperture field due to the object is proportional to the radiance $B(\tilde{u})$ at a particular point of the object.

The random coefficients of this expansion in spatial modes will be statistically independent. It is possible, therefore, to estimate the radiance $B(\tilde{u})$ at points on the object spaced by $\delta_x = \lambda R/a$ in the x-direction and by $\delta_y = \lambda R/b$ in the y-direction, and these estimates can be made independently. Conversely, it is to be expected that $B(\tilde{u})$ cannot be estimated at a finer grid of sample points by any method that does not require simultaneous calculations involving all the points.

A lower bound to the relative mean-square error of an unbiased estimate of the radiance $B_{\tilde{p}} = B(\tilde{u}_{\tilde{p}})$ at the sample point $\tilde{u}_{\tilde{p}} = (p_x \delta_x, p_y \delta_y)$ can be calculated by means of the Cramér-Rao inequality.[24-26] As might be expected, this lower bound is the same as that determined in IV for the relative mean-square error of the radiant power of a point source.

Since the number operators $n_{\tilde{p}m} = b^+_{\tilde{p}m} b_{\tilde{p}m}$ for the spatio-temporal modes commute and can be measured simultaneously, the classical-statistical form of the Cramér-Rao inequality can be used, and since the modes are statistically independent, they can be treated separately. The data for estimating $B_{\tilde{p}}$ are the observed numbers $n'_{\tilde{p}m}$ of photons in the modes $(\tilde{p}m)$, whose joint probability is, as in Eq. (2.8),

$$p(\{n'_{pm}\};\ \theta) = \prod_m (1 - v_{pm}) \exp(n'_{pm} \ln v_{pm}),$$

$$v_{pm} = N_{pm}/(1 + N_{pm}), \tag{3.1}$$

where

$$N_{pm} = \mathfrak{N} + g_m \theta \tag{3.2}$$

with $\theta = h_p N_s$ proportional to B_p through an equation like Eq.(1.21).

The mean-square error of an unbiased estimate $\hat{\theta}$ of θ is bounded below by

$$E(\hat{\theta} - \theta)^2 > \{E[\frac{\partial}{\partial\theta} \ln p(\{n'_{pm}\};\ \theta)]^2\}^{-1}$$

$$= \{\sum_m [g_m{}^2/N_{pm}(1 + N_{pm})]\}^{-1}. \tag{3.3}$$

By use of Eq. (1.15) and the inequalities

$$WT >> 1, \qquad N_{pm} << 1,$$

the sum over m can be approximated by an integral over frequency involving the spectral density $X(\omega)$ of the object light. As a result the relative mean-square error in an unbiased estimate of θ or B_p is bounded below by

$$E(\hat{B}_p - B_p)^2/B_p{}^2 \geq N_{ps}{}^{-1}[f_1(\mathscr{D}_p)]^{-1},$$

$$\mathscr{D}_p = N_{ps}/\mathfrak{N}WT, \tag{3.4}$$

where $N_{ps} = h_p N_s$ is the total average number of photons received from the object in spectral mode p, that is, from an area $A_\delta = \delta_x \delta_y$ of the object about u_p. The function $f_1(\mathscr{D})$ is the same as in IV, Eq. (3.4),

$$f_1(\mathscr{D}) = \mathscr{D}W \int_{-\infty}^{\infty} [X(\omega)]^2 [1 + \mathscr{D}WX(\omega)]^{-1}\, d\omega/2\pi, \tag{3.5}$$

and Eq. (3.4) corresponds to IV, Eq. (4.6) for the relative mean-square error in the radiant power of a point object.

When the spectral density of the object is rectangular, the total number

$$n_{\tilde{p}} = \sum_m n'_{\tilde{p}m}$$

of photons from all temporal modes in spatial mode $\tilde{p}$ is a sufficient estimator of the parameter θ or, equivalently, of the radiance $B_{\tilde{p}}$ at the sample point $u_{\tilde{p}}$ on the object.[24,26] It provides an unbiased estimate after the known average contribution $N_0 = \mathfrak{N} WT$ of the background is subtracted, and the relative mean-square error of the estimate is given by the right-hand side of Eq. (3.4), where now

$$f_1(\mathscr{D}) = \mathscr{D}/(\mathscr{D} + 1).$$

Under extreme quantum-limited conditions the minimum relative mean-square error in an estimate $\hat{B}_{\tilde{p}}$ is equal to $N_{\tilde{p}s}^{-1}$, where $N_{\tilde{p}s}$ is the average number of photons received during (0, T) from the element of area $\delta_x\delta_y$ about the point $(p_x\,\delta_x,\, p_y\,\delta_y)$. Under a background limitation $(K\mathcal{T} \gg \hbar\Omega)$, the minimum mean-square error is, as in I, Eq. (6.3),

$$\tilde{E}(\hat{B}_{\tilde{p}} - B_{\tilde{p}})^2/B_{\tilde{p}}^2 = (N'/E_{\tilde{p}s})^2\, WT,$$

where $E_{\tilde{p}s} = N_{\tilde{p}s}\hbar\Omega$ is the total average energy received from the area $\delta_x\delta_y$ about $u_{\tilde{p}}$, and $N' = K\mathcal{T}$ is the spectral density of the background light, assumed spatially and temporally white.

Appendix

Approximate Eigenvalues of a Circularly Symmetrical Kernel

Dropping the primes on the eigenfunctions in Eq. (1.20) and writing $\psi(\underset{\sim}{r})$ for $\beta(\underset{\sim}{r})/A\beta(0)$, we study the integral equation

$$h_{km}\,\eta_{km}(\underset{\sim}{r}) = \int_A \psi(\underset{\sim}{r} - \underset{\sim}{s})\,\eta_{km}(\underset{\sim}{s})\,d^2\underset{\sim}{s}, \qquad \text{(A1)}$$

in which $\psi(\underset{\sim}{r})$ is assumed to be a function of $r = |\underset{\sim}{r}|$ only. Its Fourier transform

$$\Psi(\underset{\sim}{\rho}) = \Psi(\rho) = \int \psi(\underset{\sim}{r})\,\exp(-i\underset{\sim}{\rho}\cdot\underset{\sim}{r})\,d^2\underset{\sim}{r} \qquad \text{(A2)}$$

is a function only of $\rho = |\underset{\sim}{\rho}|$. (Unmarked integrals are taken over all of two-dimensional space.) Therefore,[27]

$$\psi(\underset{\sim}{r} - \underset{\sim}{s}) = \int \Psi(\underset{\sim}{\rho})\,\exp[i\underset{\sim}{\rho}\cdot(\underset{\sim}{r} - \underset{\sim}{s})]\,d^2\underset{\sim}{\rho}/(2\pi)^2$$

$$= \int_0^\infty \rho\Psi(\rho)\,J_0(\rho|\underset{\sim}{r} - \underset{\sim}{s}|)\,d\rho/2\pi =$$

$$\sum_{m=0}^{\infty} (2 - \delta_{m0}) \int_0^\infty \rho\Psi(\rho)\,J_m(\rho r)\,J_m(\rho s)\cos m(\theta_r - \theta_s)\,d\rho, \qquad \text{(A3)}$$

where $s = |\underset{\sim}{s}|$ and θ_r and θ_s are the polar angles of the points $\underset{\sim}{r}$ and $\underset{\sim}{s}$, respectively.

We assume to start with that the eigenfunction $\eta_{km}(\underset{\sim}{s})$ is given for $m > 0$ by

$$\eta_{km}(\underset{\sim}{s}) = C_{km}\,J_m\,(b_{km}s)\cos m\theta_s, \qquad \text{(A4)}$$

where C_{km} is a normalizing constant and $x_{km} = b_{km}a$ is the k-th zero of the Bessel function $J_m(x)$; a is the radius of the aperture. It will appear later that this assumption is approximately correct when the radius a of the aperture is much greater than the width of $\psi(\underset{\sim}{r})$. A second set of eigenfunctions is, for

$m > 0, \qquad \eta_{km}(\underset{\sim}{s}) = C_{km} J_m(b_{km}s) \sin m\theta_s;$ (A5)

the derivation to follow goes through for them as well, and the resulting eigenvalues h_{km} are the same. For m = 0 the eigenfunctions are, still approximately,

$$\eta_{k0}(\underset{\sim}{s}) = C_{k0} J_0(b_{k0}s). \tag{A6}$$

Thus the eigenvalues h_{km} have multiplicity 1 for m = 0 and multiplicity 2 for m > 0. All these eigenfunctions are orthogonal over the circle $0 \le s \le a$, $0 \le \theta_s < 2\pi$.

Substituting from Eqs. (A3) and (A4) into Eq. (A1) and integrating over θ_s, we find

$$\begin{aligned} h_{km}\,\eta_{km}(\underset{\sim}{r}) &= C_{km} \cos m\theta_r \\ &\times \int_0^\infty \rho d\rho \int_0^a sds\ \Psi(\rho)\ J_m(\rho r)\ J_m(\rho s)\ J_m(b_{km}s) \\ &= C_{km} \cos m\theta_r \int_0^\infty \rho\Psi(\rho)\ F_{km}(\rho)\ J_m(\rho r)\ d\rho, \end{aligned} \tag{A7}$$

where[27]

$$\begin{aligned} F_{km}(\rho) &= \int_0^a s\ J_m(\rho s)\ J_m(b_{km}s)\ ds \\ &= (\rho^2 - b_{km}{}^2)^{-1}\ b_{km}a\ J_m'(b_{km}a)\ J_m(\rho a). \end{aligned} \tag{A8}$$

The function $F_{km}(\rho)$ is sharply peaked near $\rho = b_{km}$; its width is of the order of a^{-1}. When the width of $\psi(\underset{\sim}{r})$ is much less than a, its Fourier transform $\Psi(\rho)$ is nearly constant for changes in ρ of the order of a^{-1}. Therefore, we can put $\Psi(\rho) = \Psi(b_{km})$ in the integrand of Eq. (A7) and take it outside the integral. The integration over ρ in the first part of the right-hand side of Eq. (A7) can now be carried out; it represents the closure relation for the Fourier-Bessel transform and yields a delta function $s^{-1}\delta(r - s)$. Upon integrating over s, we get approximately

$$h_{km}\, \eta_{km}(\underset{\sim}{r}) = C_{km}\, \Psi(b_{km})\, J_m(b_{km} r) \cos m\theta_r, \tag{A9}$$

verifying our choice in Eq. (A4) of the approximate eigenfunctions. Hence $h_{km} = \Psi(b_{km})$, and translating this result into the notation of Section I, we obtain Eq. (1.24).

Acknowledgment

I wish to thank Mr. Yie-Ming Hong for programming the calculations of detection probabilities by the digital computer. I am grateful to Dr. David Slepian of the Bell Telephone Laboratories, Inc., for supplying a program to calculate the generalized prolate spheroidal wavefunctions and their eigenvalues.

Footnotes

* This research has been carried out under NASA Grant No. 05-009-079.

1. C. W. Helstrom, J. Opt. Soc. Am. 59, 164 (1969), herein referred to as I.

2. C. W. Helstrom, J. Opt. Soc. Am. 59, 331 (1969) (II).

3. D. Middleton, An Introduction to Statistical Communication Theory, (McGraw-Hill Book Co., New York, 1960), Chs. 18-22.

4. C. W. Helstrom, Statistical Theory of Signal Detection, (Pergamon Press, Ltd., Oxford, 1968), 2nd. Ed., Chs. 3, 8.

5. G. Toraldo di Francia, J. Opt. Soc. Am. 59, 799 (1969). This paper provides references to previous work on image degrees of freedom.

6. W. Louisell, Radiation and Noise in Quantum Electronics (McGraw-Hill Book Co., New York, 1964), Ch. 4.

7. Ref. 4, pp. 69-72; ref. 1, Section I.

8. C. W. Helstrom, J. Opt. Soc. Am. 59, (1969), herein referred to as III.

9. Ref. 4, Ch. 11, §1 (iii), p. 383.

10. Ref. 8, Section V and Appendix.

11. U. Grenander and G. Szegö, Toeplitz Forms and Their Applications (Univ. of California Press, Berkeley, 1958), §8.6, pp. 136-139.

12. D. Slepian and H. O. Pollak, Bell Sys. Tech. J. 40, 43 (1961).

13. See ref. 1, Eqs. (1.8), (1.9), (A2).

14. C. W. Helstrom, "Estimation of Object Parameters by a Quantum-Limited Optical System", submitted to J. Opt. Soc. Am, and herein referred to as IV. See Section IV.

15. D. Gabor, "Light and Information", Progress in Optics (E. Wolf, ed., North-Holland Publishing Co., Amsterdam), 1, 109 (1961). See p. 138.

16. D. Slepian, Bell Sys. Tech. J. 43, 3009 (1964).

17. A. Kuriksha, Radio Engrg. and Electronic Phys. 13, 1567 (1968).

18. G. Wentzel, Quantum Theory of Fields (Interscience Publishers, New York and London, 1949), Ch. I.

19. R. J. Glauber, Phys. Rev. 131, 2766 (1963), Section VIII.

20. Ref. 6, §6.10, pp. 242-245.

21. C. W. Helstrom, Trans. IEEE, IT-10, 275 (1964).

22. Ref. 4, p. 152.

23. Ref. 4, p. 219.

24. H. Cramér, Mathematical Methods of Statistics (Princeton University Press, 1946), pp. 473 ff.

25. See also I, Section VI, and IV.

26. Ref. 4, pp. 260-261.

27. Here we have used Eq. 7.3.1(2), p. 14, and Eq. 7.15(31), p. 101 in A. Erdélyi et al. (eds.), Higher Transcendental Functions (McGraw-Hill Book Co., New York, 1953), vol. 2.

28. Ref. 26, Eq. 7.14.1(9), p. 90.

Figure Caption

Fig. 1. Probability Q_d of detecting a uniform circular object of radius a_o by observations at an aperture of radius a, versus the average number N_s of photons received from the object. The average number of background photons is $N_0 = \mathfrak{N} WT = 1.0$; the false alarm probability is $Q_0 = 0.01$. The curves are indexed by the parameter $\alpha = 2\pi a a_o / \lambda R$.

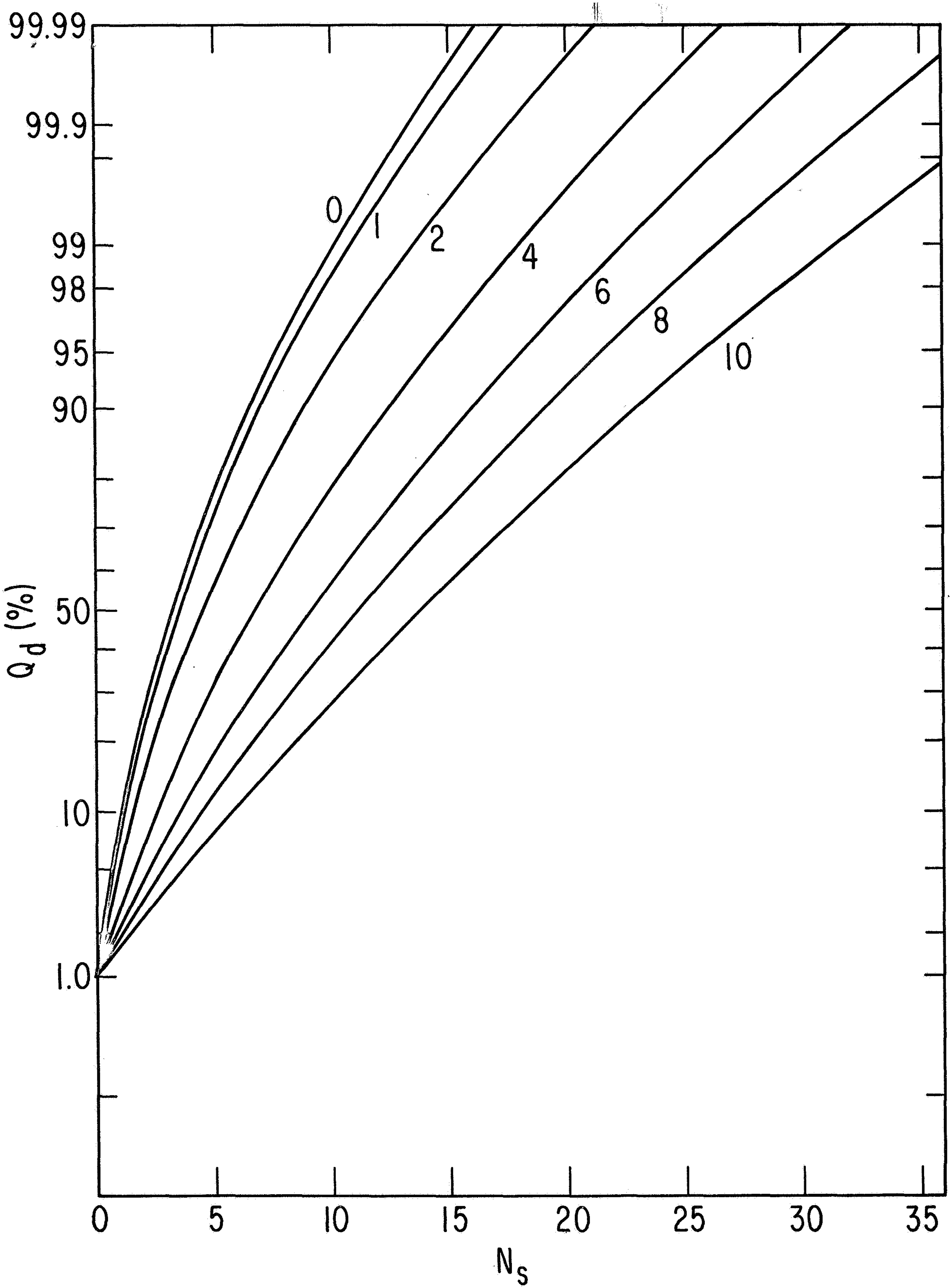
99.99
99.9
99
98
95
90
50
10
1.0
Q_d (%)
0
1
2
4
6
8
10
0
5
10
15
20
25
30
35
N_s